Results in Engineering 28 (2025) 108124

Contents lists available at ScienceDirect

Results in Engineering

journal homepage: www.sciencedirect.com/journal/results-in-engineering

Research paper

Reverse engineering of impellers to reduce pipe network pressure and enable sustainable power generation using pumps as turbines (PATs)

Ali Abdulshaheed [a,*], Faizal Mustapha, Professor [b], Shahrul Sham Dol, Professor [c], Kamarul Ariffin Ahmad, Senior Lecturee [b], Mazli Mustapha [d], Mohd Anuar, Professor [e]

[a] Dept. of Aerospace, Univ. Putra Malaysia, 43400 UPM, Serdang, Selangor, Malaysia
[b] Dept. of Aerospace, Univ. Putra Malaysia, 43400, UPM, Serdang, Selangor, Malaysia
[c] Dept. of Mechanical and Industrial Engineering, Engineering, Abu Dhabi University, Abu Dhabi, PO 59911, United Arab Emirates
[d] Dept. of Mechanical Engineering, Universiti Teknologi PETRONAS, Seri Iskandar 32610, Malaysia
[e] Dept. of Mechanical and Manufacturing Engineering, Univ. Putra Malaysia, 43400 UPM, Serdang, Selangor, Malaysia

ARTICLE INFO

Keywords:
Reverse engineering of impeller
Pump 3D design with validation
PAT performance curve
Water Network District (WDN)
Numerical Simulation of PAT model

ABSTRACT

A pump working as a turbine is a hydraulic machine type that can operate as both a pump and a turbine (PAT) by reversing the flow direction. The PAT could be an effective method for meeting global energy demands, particularly in rural and isolated areas. Furthermore, the operating costs of micro-hydropower systems are lower compared to conventional hydrodynamic turbines, although they require a high initial investment. The pump-as-turbine has been applied in various engineering fields, including irrigation, sewage, reverse osmosis, water piping networks, storage, and pressure-reducing valves. Reducing pressure in a pipe distribution system also decreases leaks within piping systems. To estimate the performance of a pump-as-turbine (PAT), the influence of pump design parameters and its best efficiency point should be identified. Current research focuses on designing a 3D centrifugal pump from scratch by applied reverse engineering for existing pump's impeller part and extract power from pipe distribution system. The extracted dimensions by reverse engineering were validated in two steps, results of pump design equations, and the result of CFTurbo software. Numerical simulations were carried out for a 3D centrifugal pump operating as a turbine at its best efficiency point in terms of velocity and head using pump to turbine transformation equations. Subsequently, simulations were conducted based on data collected from a water company, using the pump-as-turbine during low water consumption periods. This approach reduces pressure within the Seri Aman pipe distribution system, allowing for the transfer of mechanical power that could be used to produce electricity.

1. Introduction

In recent years, the demand for energy from renewable resources has increased dramatically, while natural resources like oil and fossil gas are becoming scarce [1]. Conventional green power resources, such as wind turbines, sea wave power harvesting, and solar energy technologies, are sustainable but are more expensive and complex, with higher maintenance costs. In contrast, pump as turbines (PATs) are more affordable and have lower maintenance requirements. Additionally, the availability of spare parts, the low cost of hydro plants, and their ability to operate as both pumps and turbines in reverse flow make PATs an attractive solution [2]. Their wide application range and capability to work with downstream residual pressure make them ideal for in-pipe energy recovery in existing water infrastructures [3,4]. These systems have been built all throughout the world, but they are especially popular in developing countries like East Asia and Africa [5]. In recent years, there has been a growing interest in using pumps as turbines (PATs), particularly for power supply systems in isolated places, both on and off the grid. A complete assessment of the current state of knowledge and experience in this field has been presented, Ansys Fluent software includes comprehensive models for accurately treating and simulating steady-state and turbulent flow over pipes and intricate geometries [6, 7]. The solution model must address near-wall flow and vortex formation within the geometry, which can impact fluid element velocity direction [8]. PATs are utilized for energy recovery in water distribution

* Corresponding author.
E-mail addresses: ali2007en@yahoo.com (A. Abdulshaheed), faizalms@upm.edu.my (F. Mustapha), sharulshambin.dol@adu.ac.ae (S.S. Dol), aekamarul@upm.edu.my (K.A. Ahmad), mazli.mustapha@utp.edu.my (M. Mustapha), khairol@upm.edu.my (M. Anuar).

https://doi.org/10.1016/j.rineng.2025.108124
Received 2 July 2025; Received in revised form 25 October 2025; Accepted 6 November 2025
Available online 8 November 2025
2590-1230/

Nomenclature

PATs	Pump as turbine;
WDN	Water district network;
D_1	Inlet diameter;
α_1	Inlet main flow angle;
Dshrou	Shroud impeller diameter;
Dshaft	Shaft inner Diameter;
b_2	Outer width of blade;
β_1	Inlet impeller relative angle value;
Q	Pump Flowrate;
V_r	Radial velocity;
Wu	Whirl velocity;
W	Relative velocity;
η_h	Pump efficiency;
Q_{th}	Theoretical pump flowrate;
L	Length;
V_{th}	Theoretical velocity at pump output;
d_S	Pump Suction inlet diameter;
g	Water gravitational acceleration;
σ	slip factor;
k_w	Factor;
P_t	Turbine power;
P_{tb}	Turbine Power at best efficiency point;
η_t	Turbine efficiency;
c, b, a	Pump to turbine head, flowrate convert's constant;
ω	Angular velocity;
PRVs	Pressure reduction valve;
U_1	Tangential velocity at inlet;
D_2	Outlet diameter;
α_2	Outlet main flow angle;
D_{hub}	Shaft outer Diameter;
Z	Number of impeller blade;
β_2	Outlet impeller relative angle value;
N	Impeller speed;
H	Pump head;
V	Main flow velocity;
Vu	Circumential velocity;
Nsp	Pump specific speed;
f	Pump friction coefficient;
Q_{act}	Actual pump flowrate;
D_3	First volute diameter;
d_D	Pump deliver outlet diameter;
K_3	Volute velocity constant;
P	Power;
Q_t	Turbine flowrate;
Q_{tbep}	Turbine flowrate at best efficiency point;
H_{pbep}	Pump head at best efficiency point;
H_{pbep}	Pump head at best efficiency point;
H_{loss}	Head of losses;
N_{st}	Turbine specific speed;
ρ	Fluid density;

Fig. 1. pump's impeller Ready for Reverse engineering.

networks (WDNs) and small hydropower plants [9–11]. The prediction of the transition from pump to turbine mode depends on velocity triangles, impeller angles, and the pump's best efficiency point [12–14]. Besides power generation, PATs also act as throttle valves for flow control. Furthermore, pressure reducing valves (PRVs), which typically cause mechanical dissipation of hydraulic energy, are often used to manage the pressure regime within the system and to handle topographical discontinuities along the pipeline path [15]. This helps avoid high pressures in the network, which could lead to ruptures and water leakages [16,17]. Approximately 40% of the gross energy potential available in a PRV may be recovered by replacing the valve with a PAT [5,18]. An economic assessment was included in a case study of a particular installation. The design of pumps for turbine mode is a topic that has received substantial attention [19,20]. The hydraulic behaviour of a PAT is similar to that of a Francis turbine; however, a PAT typically features a larger diameter impeller and backward-swept blades [21–23] claimed that the best performances for PATs result in pressure drops smaller than those typically produced by a PRV, with output pressure levels that ensure water delivery to consumers within the designed head limitations of the piping network [24]. proposed approximating the relative head and power curves across the processed flow rate for any given machine with second- and third-order polynomials [25]. proposed a new method to develop PAT head and power curves relative to the best efficiency point (BEP), interpolating to second- and third-degree polynomials, respectively. Research involving reverse engineering has been conducted to measure impeller design parameters and design a volute as the second part of a simulated 3D centrifugal pump model. The design parameter equations were described by [26–29]. Additionally, the new 3D model was validated by establishing design parameters within CFTurbo software, with the goal of ensuring accuracy for impeller angles, velocity triangles, and volute design. Model performance curves were plotted. A key aspect of understanding PAT performance is analyzing and estimating pump design parameters and their relation to performance curves. Illustrating the transformation equations from pump to turbine helps compare these performance curves. The contribution of this research lies in recreating PAT model from pump's impeller scratch through reverse engineering result in extracting power from a pipe distribution network. The approach includes extracting design parameters of the pump's impeller part by reverse engineering (Fig. 1) and design volute according to the extracted parameters. In addition, validate extracted impeller and volute parameters (predicted through impeller parameters and volute design equation) in two steps, result of pump design equations, and CFTurbo software result using same design parameters. The validation includes impeller design parameters value (Table 1), velocity triangles value (Table 1, Fig 7), and volute design parameters (Fig 5). Furthermore, the robust parameter of the pump would be used to create a 3D model using CATIA software. presenting a pump performance curve and defining transformation equations for the pump operating in reverse direction (PAT) to print PAT

Table 1
The Pump Design Parameter.

Impeller Design Dimensions	Impeller Design Parameters	Value	UNIT
Inlet main flow angle	α_1	90°	degree
Inlet impeller relative angle value	β_1	18°	degree
Shroud impeller diameter	D_{shroud}	120	mm
Outlet impeller diameter	D_2	250	mm
Outlet main flow angle	α_2	7.6°	degree
Outlet impeller relative angle value	β_2	9.5°	degree
Impeller speed	N	1450	RPM
Pump Flowrate	Q	60	M^3/h
Pump head	H	20	M
Shaft inner Diameter	D_{shaft}	30	mm
Shaft outer Diameter	D_{hub}	40	mm
Outer width of blade	b_2	17.2	mm
Number of impeller blade	Z	6	–

performance curves. The comparison between power extracted theoretically and by Ansys simulation intended to validate the simulation results, The importance of the solutions model used lies in its applicability to solve fluid flow near walls (share stress) and the creation of vortices and its challenge of boundary condition as important requirement for software validation, which can change the flow state from laminar to turbulent even at low Reynolds number values. The limitation of flow depending on the Reynolds number was overcome when the solution model predicted that viscous forces could dominate the flow. Extracting transformed torque using the 6 DOF method depends on angular velocity and rotor moment of inertia (calculated using Catia software). In addition, expression option was applied to get angular velocity through dividing linear velocity by PAT's rotor radius. Finally, the established model functions as a turbine and is conducted to reduce the pressure value of the Seri Aman pipe distribution network by using Ansys software setup which validate previously, the extracted energy during periods of low water consumption, pipe network data obtained from [30].

2. Design of the pump theory and numerical analysis

The impeller is the part of the pump responsible for delivering and accelerating fluid by transferring energy from a diesel or electric motor. To understand impeller design and enhance research reliability, a closed impeller model was selected to measure all design parameters, as shown in Fig. 1, internal diameter (D_1), outer diameter (D_2), the angle of the impeller blade in a plane parallel to D_1 (β_1), and the angle of the impeller blade in a plane perpendicular to D_1 (α_1). Similarly, the angle of the impeller blade in a plane parallel to D_2 (β_2) and the angle of the impeller blade in a plane perpendicular to D_2 (α_2) were also measured.

2.1. Measuring design parameters for impeller model

Reverse engineering has been carried out. Moreover, tools are used to measure angles and length. Reverse engineering was conducted, and various tools were used to measure the angles and lengths accurately. It was essential to section the impeller to measure inner blade parameters, which are critical for simulating the blade's inner curve and twist, the sketch of dimensions was illustrated in Fig 2 and 3.

The impeller suction is cut through two stages. First, a welding machine is used due to the thick shaft and base impeller zone, which exceeds the capacity of local laser cutting machines. Second, a cutter tool is used for the cover and shroud zones.

The design parameters are as below in Table 1.

2.2. Design pump's volute

The second important part of the centrifugal pump is called the volute (case), which serves as a cover for the pump's impeller. The impeller rotates to impart power to the fluid inside the volute. The fluid enters the volute through the inlet and is delivered to the pumping system through the outlet. The angle between the pump's inlet and

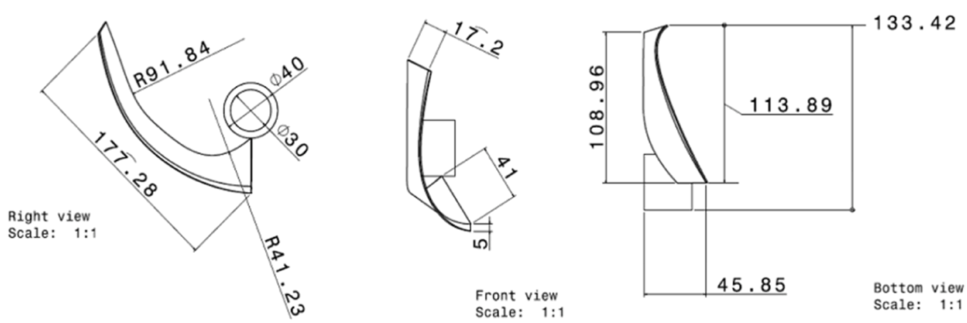

Fig. 2. Impeller Blade Dimensions.

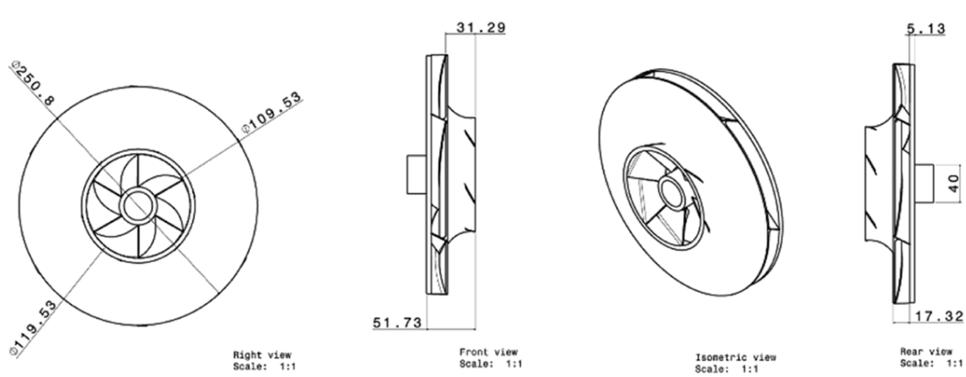

Fig. 3. Pump impeller Dimensions.

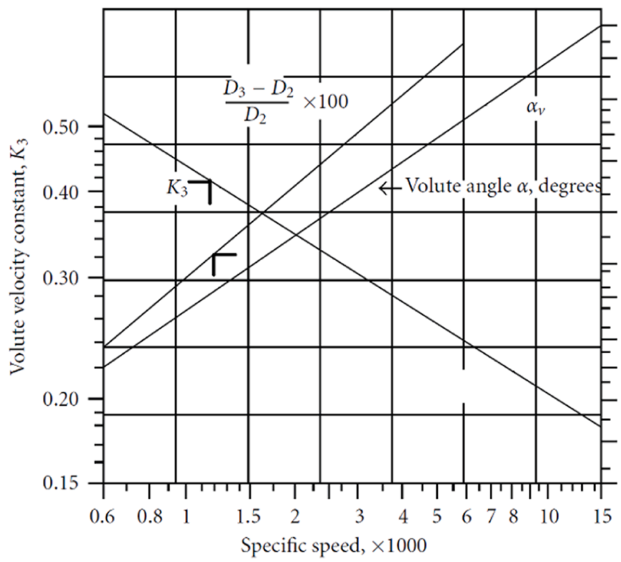

Fig. 4. volute velocity constant chart.

Table 2
Theoretical Impeller design Velocities value.

NO	Impeller Velocities	Parameters	Pump inlet value	Pump outlet value	UNIT
1	Radial velocity	V_r	2	1.4	m/s
2	Main Flow velocity	V	2	10.6	m/s
3	Peripheral velocity	U	6.1	18.9	m/s
4	Whirl velocity	W_u	6.1	8.5	m/s
5	Circumferential velocity	V_u	0	10.4	m/s
6	Relative velocity	W	6.5	8.6	m/s
7	Absolute flow angle	α	90°	7.6°	degree
8	Relative angle	β	18°	9.5°	degree
9	slip	σ	-	0.88	degree

outlet is 90°, and the diameter of the volute increases toward the pump's outlet to convert kinetic energy into pressure energy. In contrast, when the pump operates in reverse flow as a turbine (PAT), the fluid enters from the pump outlet and flows toward the inlet, as shown in Fig. 4.

$$d_S > d_D \tag{1}$$

because α_1 equal to 90° led to the equation for calculation volute through value as below.

$$\beta 1 = \tan^{-1}[\frac{V_1}{U_1} \tag{2}$$

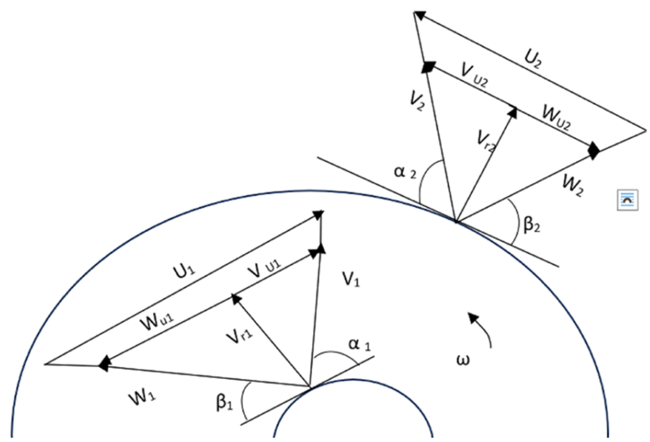

Fig. 6. Pump velocity Tringle.

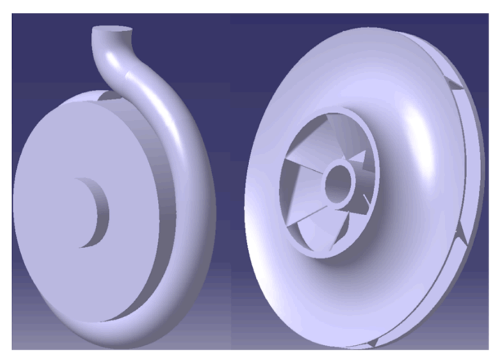

Fig. 7. volute and impeller 3D in CATIA software.

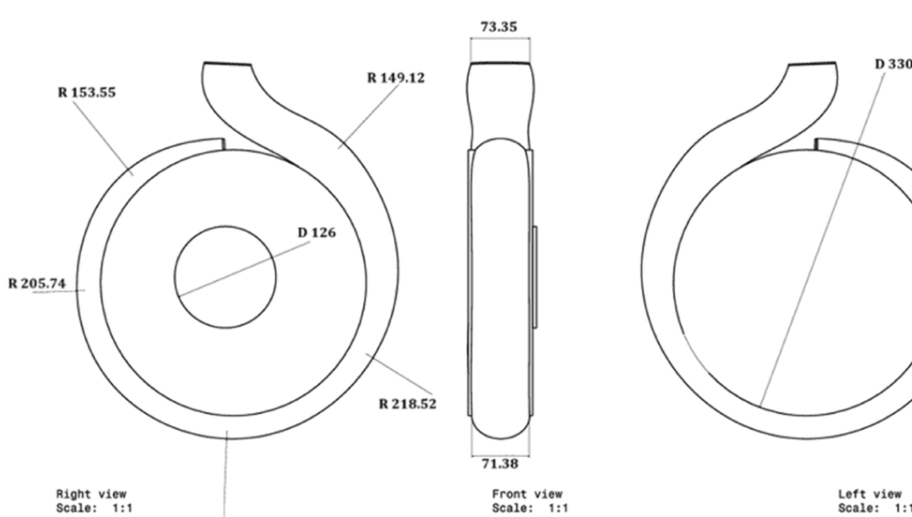

Fig. 5. Pump Volute Dimensions.

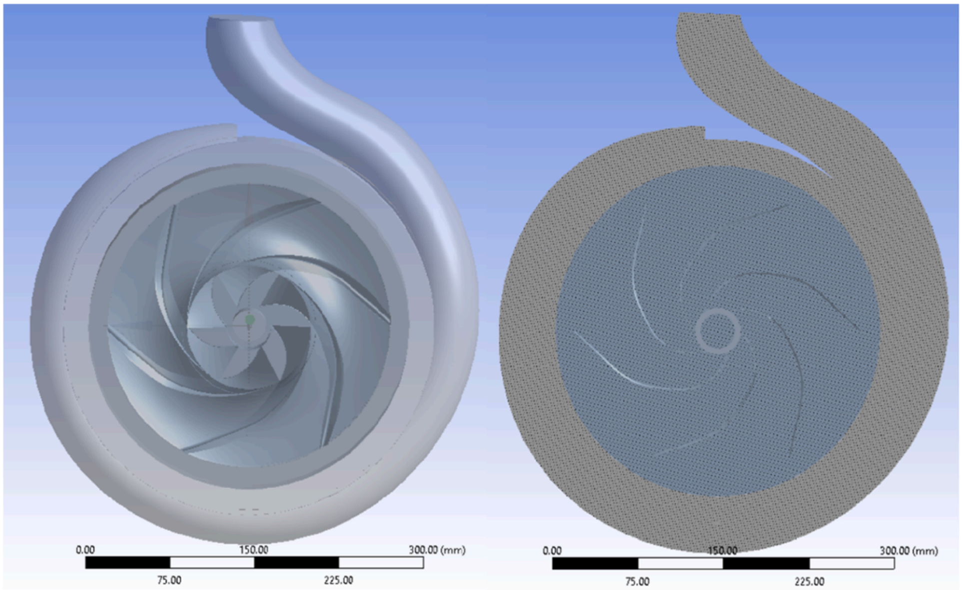

Fig. 8. Impeller and Volute in one geometry using Boolean tool.

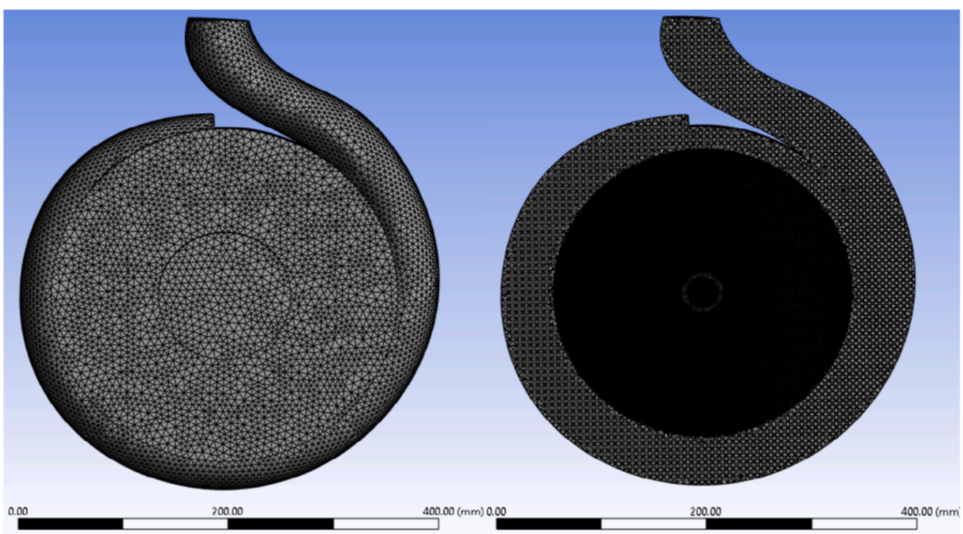

Fig. 9. Pump's Impeller and Volute mesh in Ansys Program.

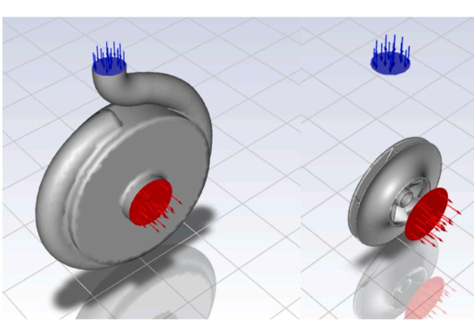

Fig. 10. PAT inlet and outlet zone.

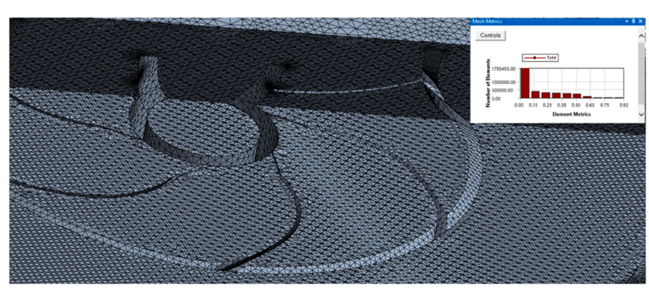

Fig. 11. Mesh skewness value result.

$$U_1 = \frac{\pi\, ND_1}{60} \tag{3}$$

$$U_2 = \frac{\pi\, ND_2}{60} \tag{4}$$

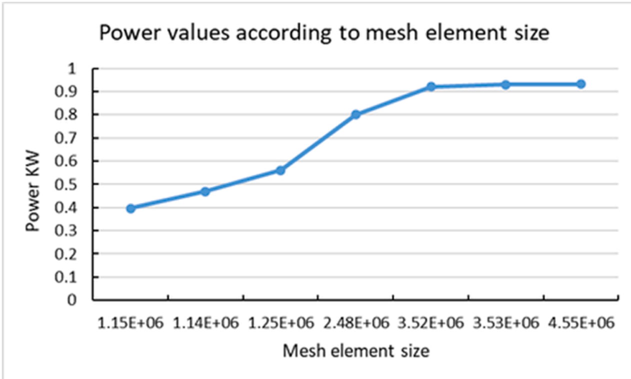

Fig 12. Output power of model according to number of mesh element.

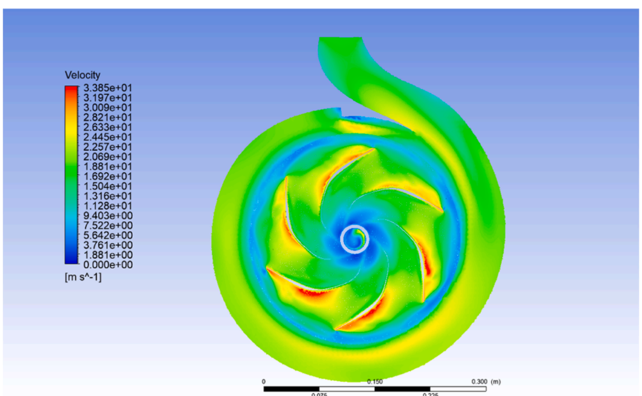

Fig. 13. Convergence PAT result at boundary conditions velocity 7.9 m/s, head 44 m.

$$\eta_h = \frac{Q_{act}}{Q_{th}} \tag{5}$$

$$N_{sp} = \frac{N\sqrt{Q}}{H^{\frac{3}{4}}} \tag{6}$$

To determine the basic parameters of pump volute design, Stepanoff's theory has been applied, with support from charts. figure out the equation constant value as seen in Fig. 4.

Head loss of fluid in the pump is calculated through the equation below

$$H_{loss} = f\frac{L}{D}\frac{V^2}{2g} \tag{7}$$

$$\text{Ratio} = \frac{D_3 - D_2}{D_2} \times 100 \tag{8}$$

where D_2 is an outer impeller diameter, D_3 is first pump's volute diameter

$$V_{th} = K_3\sqrt{2gH} \tag{9}$$

From volute velocity constant Fig. 4, at specific speed value N_s (19.8), K_3 value has extracted (0.44).

From pump's specification the pump efficiency value is (80).

$$\eta = \frac{Q_{actual}}{Q_{theoretical}} \tag{10}$$

$$Q_{theoretical} = V_{th} \times \frac{\pi d_{th}^2}{4} \tag{11}$$

$$d_{th} = \sqrt{\frac{\frac{Q_{th}}{\pi V_{th}}}{4}}$$

$$d_{th} = \sqrt{\frac{Q_{th}}{\frac{\pi V_{th}}{4}}} \tag{12}$$

2.3. Design of the impeller theory and numerical analysis

This research includes an additional step to validate the pump's impeller model by building a new model in the software and simulating it as designed in CATIA. The models are then matched in the CFTurbo program to ensure the reliability of the impeller model dimensions. A trusted design supports successful simulation results, with all fluid velocities inside the impeller, generated by its rotation direction and impeller angles. Pump's velocity tringle is depicted in Fig. 6.

When the pump impeller is in operation, slip at the impeller angles is noted. This reduction in angle value, which alters pump impeller velocities, can lead to deviations in pump output head and discharge. Slip at the impeller's trailing edge is calculated using the GÜLICH/ WIESNER equations.

$$\sigma = f_1\left[1 - \frac{\sqrt{\sin\beta_{2b}}}{Z^{0.7}}\right]k_w \tag{13}$$

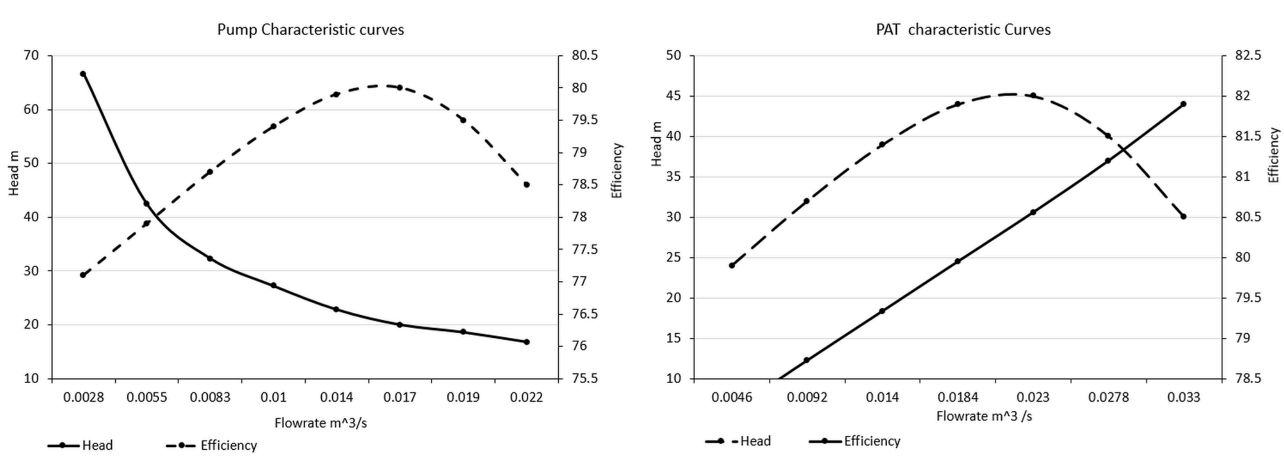

Fig. 14. characteristics curve of designed pump and pump as turbine (PAT).

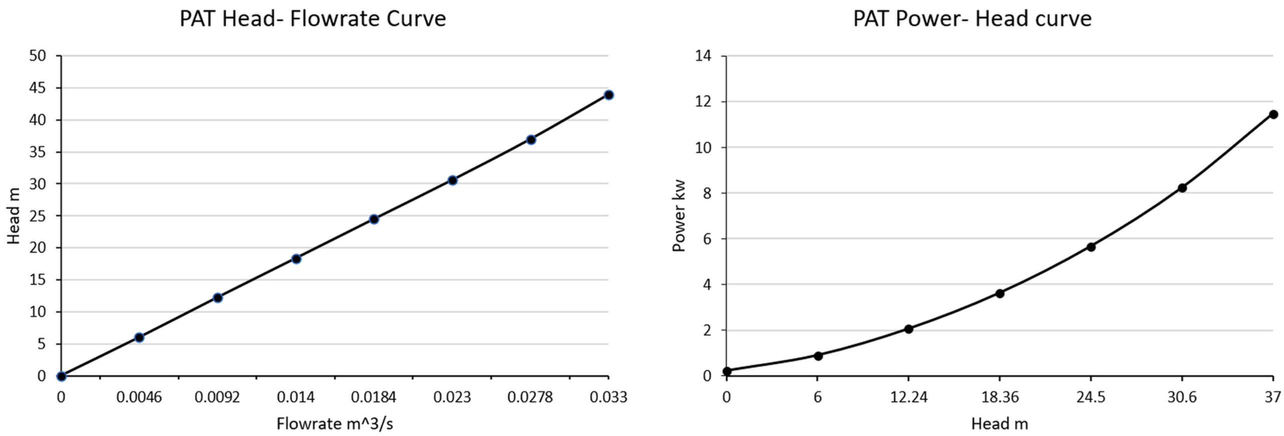

Fig. 15. Power and Head curves according to the Flowrate.

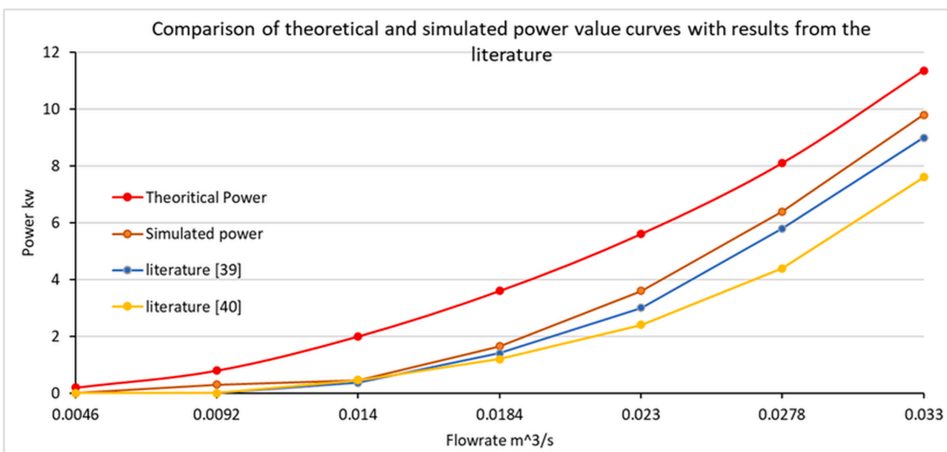

Fig. 16. Theoretical and Simulation PAT power curve comparison.

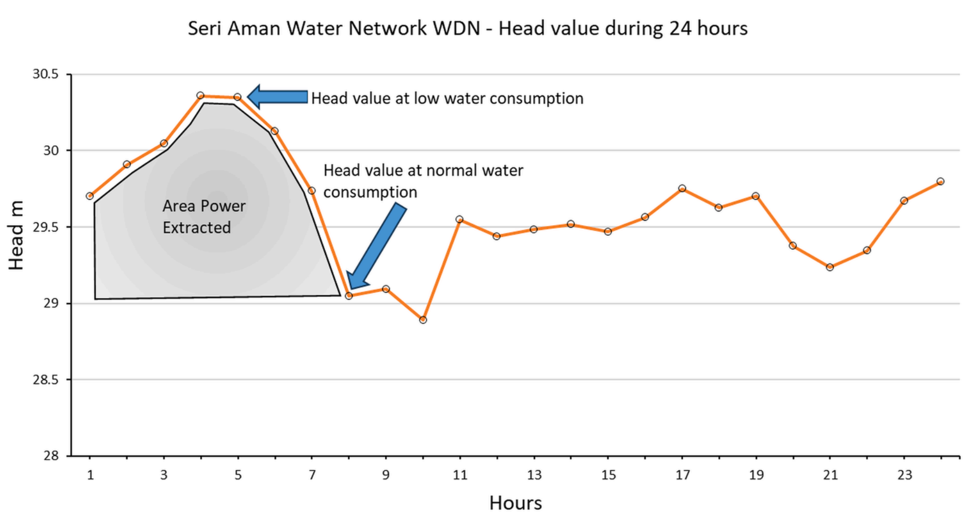

Fig. 17. Power extracted from Seri Aman WDN during low water consumption value.

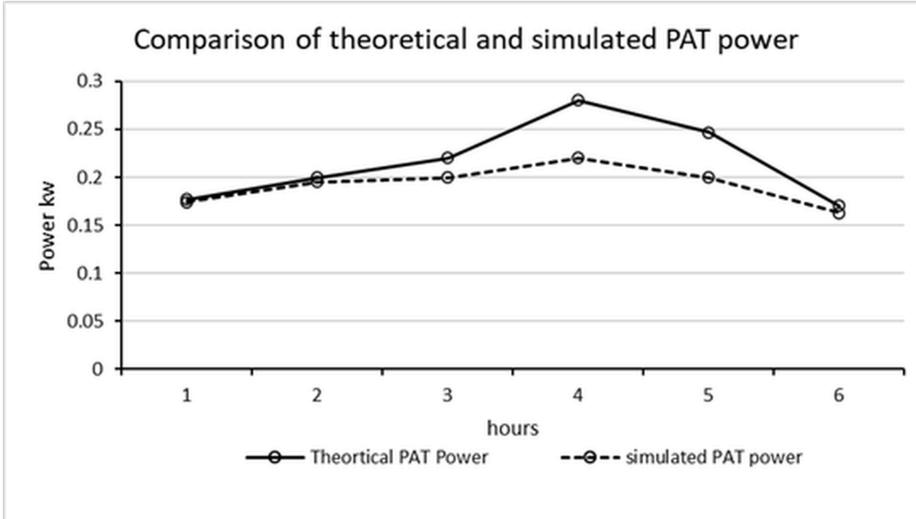

Fig. 18. comparison Theoretical and simulation PAT Power.

Table 3
Seri Aman (WDN) Pressure and Flowrate result in Simulation Torque and Angular Velocity from PAT.

NO	Flowrate (m^3/s)	Head (m)	Power (kw)	Torque (N.m)	Angular Velocity (rad/s)	Power (kw)
1	0.0315	0.7	0.177	4.6	38	0.174
2	0.029	0.9	0.2	5	39	0.195
3	0.0285	1	0.22	5.12	39	0.2
4	0.028	1.3	0.28	5.6	39	0.22
5	0.028	1.1	0.247	5.16	39	0.2
6	0.0285	0.7	0.17	4.3	38	0.163

$f_1 = 1$for radial impeller

$$\left\{\begin{array}{c} 1\text{for}d_1m/d_2 \leq \mathscr{E}_{lim} \\ k_w 1 - \left\{\dfrac{d_{1m}/d_2 - \mathscr{E}_{lim}}{1 - \mathscr{E}_{lim}}\right\}^3 \\ d_{1\mathrm{m}} = \sqrt{0.5\left(d_{1hub}^2 + d_{1shroud}^2\right)} \end{array}\right\} \tag{14}$$

$$\mathscr{E}_{lim} = \exp\left[\frac{8.16\sin\beta_{2b}}{Z}\right] \tag{15}$$

$$s_{\beta 2} = 0.5\left(s_{\beta 2hub} + s_{\beta 2shroud}\right) \tag{16}$$

The equations of impeller velocities parameters are shown (16-20).

$$V_{u2} = \frac{\mathrm{H\ g}}{U_2} \tag{17}$$

$$V_{r1} = \frac{Q}{\frac{\pi}{4}\left(d_s^2 - d_h^2\right)} \tag{18}$$

$$V_{r2} = \frac{Q}{\pi b_2 d_2} \tag{19}$$

$$W_u = U_2 - V_{u2} \tag{20}$$

$$W_2 = V_{r2}\sec\beta_2 \tag{21}$$

Theoretical Impeller angle and velocities is explained in Table 2.

Due to impeller angle blockage caused by rotational liquid flow, the impeller angle values vary, resulting in changes in impeller velocity values. The GÜLICH/ WIESNER slip method is applied in Eqs. (13-16), primarily for the outer angles (β_2 and α_2).

2.4. Pump performance curve calculations

The characteristics curve of the pump has been estimated through Affinity equation.

$$\left(\frac{Q_2}{Q_1}\right)^{\frac{1}{3}} = \left(\frac{N_1}{N_2}\right)^{\frac{2}{3}}\left(\frac{H_2}{H_1}\right)^{\frac{1}{2}} \tag{22}$$

Q pump flowmeter in m^3 /s, H is pump head in m, N was the pump specific speed.

Although, the equation of estimating power could be extracted in case of using pump as turbine as explained in the equation below.

$$P = \rho g Q H \tag{23}$$

where P is power, ρ is water density, g is gravitational acceleration, Q is pump discharge

H is total head.

2.5. Pump to turbine (PAT) transformation and performance curve calculations

In context of relations between different parameters of pump and pump working as turbine

Efficiency relation is important to estimate output and inlet power.

$$\eta_t = \eta_p + 2\ \% \tag{24}$$

Specific speed pump-turbine has linear relationship, so that values can be calculated using equation below.

$$N_{sp} = 1.125N_{st} + 1.73 \tag{25}$$

Considering N_{st} turbine specific speed, N_{sp} pump specific speed

Head discharge can be estimated by conducting [31] Eqs. (26,27).

$$\frac{H_{tbep}}{H_{pbep}} = \frac{b}{\eta^a} \tag{26}$$

$$\frac{Q_{tbep}}{Q_{pbep}} = c\ \frac{b^{0.5}}{\eta^{a/2}} \tag{27}$$

where H_t is turbine head, H_p pump head, Q_t head discharge, Q_p pump discharge, $a = c = 1.1$, $b = 1.2$

The power curve estimation, in the case of the pump operating as a turbine, is based on relationships described as third- and second-order expressions, as noted in [9]

$$\frac{P_t}{P_{tb}} = 0.3902\left(\frac{Q_t}{Q_{tbep}}\right)^3 + 2.1472\left(\frac{Q_t}{Q_{tbep}}\right)^2 - 0.8865\left(\frac{Q_t}{Q_{tbep}}\right) + 0.0452 \tag{28}$$

P_t is considered as turbine power, P_{tbep} is power of turbine at best efficiency point, $\left(\frac{Q_t}{Q_{tbep}}\right)$ ratio between turbine flowrate to the turbine flowrate at best efficiency point

$$\eta_t = \frac{T \times \omega}{\rho Q H g} \tag{29}$$

2.6. Draw 3D Impeller and Volute in Catia Program

The dimensions of the pump parts are ready to be modelled in CATIA software, one of the leading tools for mechanical design. The pump's impeller is drawn using the generative shape design mode, based on dimensions extracted from a commercial impeller. Additionally, the mechanical design mode is used to define the thickness of the solid parts. Although each solid part is modelled as a separate body in the software, the Boolean tool is applied to assemble these solid parts into a single geometry. In contrast, the volute is also designed and modelled in CATIA software using the mechanical design mode.

2.7. Numerical scheme Analysis for Pump work as Turbine and validation

The pump impeller and volute design were completed using CATIA software. Numerical analysis was then carried out in ANSYS Fluent software, using the SST k-omega model. The geometry mesh, which is highly complex and time-consuming, plays a crucial role. Since the impeller and volute geometries are assembled together, one part is considered a standard wall, while the impeller is set as a rigid wall. To simulate the actual setup, the Boolean option is applied to create a contact zone between the two parts (walls), as shown in Fig. 8.

To model the pump-as-turbine (PAT) setup, in which the pump operates in reverse flow, the impeller rotates due to water pressure and velocity values. Since the impeller speed is initially unknown, the dynamic mesh option is employed in ANSYS Fluent, using the six DOF dynamic mesh method for the impeller wall, while using remeshing technique for volute walls to enhance first node distance. Different mesh types were applied to the pump parts, the rotating zone (contact area between the volute and impeller), and the pump's volute, as illustrated in Fig. 9.

Furthermore, the inlet and outlet were defined in the geometry category within ANSYS Fluent. The pump's inlet serves as the outlet in the PAT configuration, while the pump's outlet functions as the PAT inlet. As illustrated in Fig. 10

In this context, the boundary condition at the inlet was velocity-based, while the outlet condition was pressure-based. The turbulent kinetic energy and specific dissipation rate were calculated using the second-order upwind scheme of the finite volume method. Additionally, the solution for pressure and velocity was set to SIMPLE, and the activation of the pseudo-time method ensured acceptable residual convergence 10^{-5} consider cases complexity and using dynamic mesh approach. The time step size required for convergence was 0.0009, with 200 time steps and 12 iterations per time step the convergence velocity results as shown in Fig. 13. A tetrahedral mesh type was used with a maximum skewness value of 92 and 3,520,234 elements as illustrated in Fig. 11. The volute comprised 1520000 mesh elements and the rotor zone was 2000000 mesh elements. The dimensionless y+ value for PAT model 8.13, the rotor value was 2 and the volute equal to 6.67. An independence mesh test was applied to ensure case convergence and robust results. The convergence results from the independence mesh test printed in Fig. 12. The power extracted value changes with mesh element size of the model.

The impeller rotates clockwise, with angular velocity, torque, and pressure calculated around and within the impeller, rotating zone, and volute. Torque and angular velocity depend on the power extracted from the water (fluid).

$$\mathrm{P} = T \times \omega \tag{30}$$

The torque and force report had extracted, angular velocity value was got by identify point in the rotation axis.

3. Results

The PAT's impeller was created based on reverse engineering of a commercial model, and all pump components were designed using CATIA software. The design parameter values, triangle velocities, and lead and trail angle values are illustrated in Tables 1 and 2. One challenge faced was exporting these parts as solid models into the ANSYS program, given the complexity of the impeller and volute designs. Additionally, Eqs. (1-11) were used to design the pump's volute (case), as shown in Fig. 5. The chart in Fig. 4 was then used to calculate the volute velocity constant (K_3) and the value of $\left(\frac{D_3 - D_2}{D_2}\right)$ which was used in Equation (8) to calculate (D_3) based on the specific speed value obtained from Eq. (6), D_3 is important for estimating the first diameter value of the volute. The pump and PAT (Pump as Turbine) specification curve is plotted in Fig. 14 and 15. Furthermore, the pump characteristic curve was predicted using the affinity pump Eq. (22). The 3D design was imported into ANSYS after being built in CATIA software. Various mesh types and sizes were applied to the PAT components (volute, impeller, and rotating zone) in ANSYS. The general setup was transient due to the complexity of the geometry and unknown variables. The simulation model used the SST k-omega model,

The power extracted by the PAT was determined from the fluid moving downstream from the inlet of the PAT (pump working in reverse direction) to the outlet. Moreover, a dynamic mesh was generated to simulate the impeller's rotation. A six-degree-of-freedom (DOF) dynamic mesh was implemented to define the rotation of the PAT's rotor. The identification of the PAT rotor's rotation about x axis allowed the estimation of the energy extracted from the water by the rotating part of the PAT, as expressed in Equation (30).

In terms of pump parameters, the efficiency of the pump was 80%, which means the percentage of power output relative to power input, as calculated by Equation (10). As a result, the diameter of the volute (d_{th}) was estimated. The head losses were computed using Equation (7). As fluid flows from the inlet to the outlet under specified boundary conditions, depicted in transition equations from the pump to the turbine (26,27), the potential energy of the fluid increases as it moves downward due to gravity. The velocity of the fluid stream in the PAT increases from the inlet to the outlet as the volute diameter decreases, with the maximum fluid velocity occurring at the turbine rotor. Additionally, the fluid velocity within the rotor blade increases as the fluid stream area decreases and due to the velocity differential between the rotor's inlet and outlet diameters, resulting from the transferring energy to the rotor as angular velocity and torque as seen in Fig. 13. The angular velocity of the PAT rotor is determined using the momentum equation, where it equals the product of angular velocity and moment of inertia. The transferred momentum value is the difference between the inlet and outlet fluid momentum passing through the PAT rotor, while the moment of inertia indicates resistance to rotor movement around an axis.

The characteristics of the designed centrifugal pump, operating both in pump mode and turbine mode, are illustrated in Fig. 14. The pump efficiency value was estimated using Equation (10), while the power curve was calculated using Equation (23). Furthermore, the PAT efficiency and power were computed by Eqs. (24,29) The relationship between PAT power and head, which is linear, is illustrated in Fig. 15.

Simulation was carried out using ANSYS Fluent to imitate the pump working as a turbine, using the designed 3D model as described in the section "Draw 3D Impeller and Volute in CATIA Program." Moreover, the power extracted was calculated using Equation (30).

The output of the simulation, shown in Fig. 16, indicates a zero power value at a flow rate of 0.0046. The power value increases starting at a flow rate of 0.0092. This behaviour is due to the second-order momentum equation, which results in a second-order output moment and a trending polynomial curve type (behaviour of Eq. (28)), as well as the output power.

Furthermore, the simulation was carried out based on pressure and flow rate data (boundary conditions) measured from Puncak Niaga Water Company during the hours of low water consumption (4:00 AM to 7:30 AM) as printed in Fig. 17. The pressure and flow values for the Seri Aman water network over one day were considered as the inlet boundary conditions for the existing pump working as a turbine. The pressure value was assumed to correspond to the head difference between 4:00 AM and 7:30 AM (when customer consumption is low).

The comparison between the theoretical and simulated power extracted from the Seri Aman pipe network is illustrated in Fig. 18. The theoretical and numerical power extracted was calculated using Equations (24) and (10). The pressure and flow rate values were taken from the water distribution system, as shown in Table 3.

The results show a prominent opportunity to save Power from WDN by using PAT instead of the PRV. However, PAT can be used in case of emergency as alternative power sources to keep surveillance and necessary rescue action.

4. Conclusions

The importance of this research lies in addressing the shortage of fossil fuels and the rising demand for power. The study involved the design of a 3D centrifugal pump model by applying reverse engineering to the impeller. Additionally, theoretical calculations for all triangle velocities and impeller angles were performed, and a 3D pump case model (volute) was designed, preparing the centrifugal pump model for simulation. For reliable design validation, the model was compared with one designed in CFTurbo, based on impeller reverse engineering data. To complete the 3D pump model, pump performance curves were generated. Once the 3D pump model was completed, it was further tested as a pump operating in turbine mode, identified by the performance curves. Simulation was carried out using the ANSYS program, and boundary conditions were calculated using the best efficiency point method. The proposed PAT was tested, and the theoretical and simulated power values were compared, as shown in Fig. 15. The purpose of the 3D-designed PAT model is to extract power from the Seri Aman Water Distribution Network (WDN) instead of using a Pressure Regulation Valve (PRV) during low water consumption periods. The 3D PAT model successfully extracted power from the Seri Aman WDN during this period, which would otherwise be wasted in the case of a PRV used to control pressure and flow, reducing the risk of pipe network leaks.

CRediT authorship contribution statement

Ali Abdulshaheed: Writing – review & editing, Writing – original draft, Visualization, Validation, Software, Methodology, Formal analysis, Data curation, Conceptualization. **Faizal Mustapha:** Supervision, Methodology, Investigation. **Shahrul Sham Dol:** Supervision, Methodology, Investigation. **Kamarul Ariffin Ahmad:** Validation, Software, Methodology. **Mazli Mustapha:** Writing – review & editing, Visualization, Resources. **Mohd Anuar:** Formal analysis, Data curation, Conceptualization.

Declaration of competing interest

The authors declare that they have no known competing financial interests or personal relationships that could have appeared to influence the work reported in this paper.

Data availability

Data will be made available on request.

References

[1] S. Ebrahimi, A. Riasi, A. Kandi, Selection optimization of variable speed pump as turbine (PAT) for energy recovery and pressure management, Energy. Convers. Manag 227 (2021), https://doi.org/10.1016/j.enconman.2020.113586.

[2] X. Yu, J. Zhang, D. Miao, Innovative closure law for pump-turbines and field test verification, J. Hydraul Eng. 141 (2014) 2–11, https://doi.org/10.1061/(asce)hy.1943-7900.0000976.

[3] G.A. Caxaria, D. de Mesquita e Sousa, HM. Ramos, Small scale hydropower: generator analysis and optimization for water supply systems, in: Proc World Renew Energy Congr – Sweden, Linköping, Sweden 57, 2011, pp. 1386–1393, https://doi.org/10.3384/ecp110571386, 8–13 May2011.

[4] A. Carravetta, O. Fecarotta, HM. Ramos, A new low-cost installation scheme of PATs for pico-hydropower to recover energy in residential areas, Renew Energy 125 (2018) 1003–1014, https://doi.org/10.1016/j.renene.2018.02.132.

[5] e. Souza DES, A.L.A. Mesquita, C.J.C. Blanco, Pump-as-turbine for energy recovery in municipal water supply networks. A review, J. Brazilian. Soc. Mech. Sci. Eng. 43 (2021), https://doi.org/10.1007/s40430-021-03213-z.

[6] W. Rodi, Turbulence modeling and simulation in hydraulics: A historical review, J. Hydraul Eng. 143 (2017) 1–20, https://doi.org/10.1061/(asce)hy.1943-7900.0001288.

[7] S. Kadia, I. Albayrak, L. Lia, N. Rüther, E. Pummer, Reynolds Stress model study comparing the secondary currents and turbulent flow characteristics in high-speed narrow open channel and duct flows, J. Hydraul Eng. 150 (2024) 1–17, https://doi.org/10.1061/jhend8.hyeng-13837.

[8] X. Song, X. Sun, Y. Li, J. Ma, X. Yang, Exploration of the circumferential velocity structure induced by guide vane-type spiral flow generators in a pipe flow, J. Hydraul Eng. 149 (2023), https://doi.org/10.1061/jhend8.hyeng-13495.

[9] F. Pugliese, F. De Paola, N. Fontana, M. Giugni, G. Marini, Experimental characterization of two pumps As turbines for hydropower generation, Renew Energy 99 (2016) 180–187, https://doi.org/10.1016/j.renene.2016.06.051.

[10] A.M. Abu-Mahfouz, Y. Hamam, P.R. Page, K.B. Adedeji, A.O. Anele, E. Todini, Real-time dynamic hydraulic model of water distribution networks, Water (Switzerland) 11 (2019) 1–13, https://doi.org/10.3390/w11030470.

[11] C.A.M. Ávila, F.J. Sánchez-Romero, P.A. López-Jiménez, M. Pérez-Sánchez, Improve leakage management to reach sustainable water supply networks through by green energy systems. Optimized case study, Sustain Cities Soc 83 (2022), https://doi.org/10.1016/j.scs.2022.103994.

[12] Ø. Albert, Pump as Turbine Symmetry Prediction Method for Pump as Turbine Characteristics Sondre, Norwegian University of Science and Technology |, 2018.

[13] M. Stefanizzi, M. Torresi, B. Fortunato, SM. Camporeale, Experimental investigation and performance prediction modeling of a single stage centrifugal pump operating as turbine, Energy Procedia 126 (2017) 589–596, https://doi.org/10.1016/j.egypro.2017.08.218.

[14] Liu M, Tan L, Cao S. Theoretical model of energy performance prediction and BEP ACCEPTED MANUSCRIPT determination for centrifugal pump as turbine 2019.

[15] N.B. Gorev, V.N. Gorev, I.F. Kodzhespirova, I.A. Shedlovsky, P. Sivakumar, Discussion of "head-drop method for the modeling of pressure reducing valves and variable speed pumps in water distribution networks, J. Hydraul Eng 150 (2024) 1–2, https://doi.org/10.1061/jhend8.hyeng-13702.

[16] 1 O. Fecarotta, A. Carravetta, CFD and comparisons for a pump as turbine: mesh reliability and performance concerns O, J. Energy 1 (2010) 427–446.

[17] C. Covelli, L. Cimorelli, L. Cozzolino, Morte R Della, D. Pianese, Reduction in water losses in water distribution systems using pressure reduction valves, Water Sci. Technol Water Supply 16 (2016) 1033–1045, https://doi.org/10.2166/ws.2016.020.

[18] T. Lydon, P. Coughlan, A. Mcnabola, Pressure management and energy recovery in water distribution networks: development of design and selection methodologies using three pump-as-turbine case studies, Renew Energy (2017), https://doi.org/10.1016/j.renene.2017.07.120.This.

[19] M. Rossi, A. Nigro, M. Renzi, Experimental and numerical assessment of a methodology for performance prediction of Pumps-as-Turbines (PaTs)operating in off-design conditions, Appl. Energy 248 (2019) 555–566, https://doi.org/10.1016/j.apenergy.2019.04.123.

[20] T. Lydon, P. Coughlan, A. McNabola, Pump-As-turbine: characterization as an energy recovery device for the water distribution network, J. Hydraul Eng 143 (2017), https://doi.org/10.1061/(asce)hy.1943-7900.0001316.

[21] D. Novara, A. McNabola, A model for the extrapolation of the characteristic curves of Pumps as turbines from a datum Best Efficiency point, Energy Convers Manag 174 (2018) 1–7, https://doi.org/10.1016/j.enconman.2018.07.091.

[22] A.A. Bideris-Davos, PN. Vovos, Algorithm for appropriate design of hydroelectric turbines as replacements for pressure reduction valves in water distribution systems, Water (Switzerland) 15 (2023), https://doi.org/10.3390/w15030554.
[23] A.A. Bideris-Davos, PN. Vovos, Techno-economic design and placement tool for energy recovering pressure regulating turbines in water distribution systems, Renew Energy 237 (2024), https://doi.org/10.1016/j.renene.2024.121460.
[24] S. Derakhshan, A. Nourbakhsh, Experimental study of characteristic curves of centrifugal pumps working as turbines in different specific speeds, Exp. Therm. Fluid. Sci. 32 (2008) 800–807, https://doi.org/10.1016/j.expthermflusci.2007.10.004.
[25] Novara D, McNabola A. The development of a decision support software for the design of micro-hydropower schemes utilizing a pump as turbine 2018:678. https://doi.org/10.3390/proceedings2110678.
[26] Stepanoff AJ. Centrifugal and axial flow pumps. 1957.
[27] Jacobs BEA. Rotodynamic pumps. 2020. https://doi.org/10.1201/9781482296600-15.
[28] KARASSIK IJ, KRUTZSCH WC, FRASER WH, MESSINA JP. Pump Handbook. 1976.
[29] Gülich JF. Cenerifugal pumps. 2016.
[30] A. Abdulshaheed, F. Mustapha, M. Anuar, Pipe material effect on water network leak detection using a pressure residual vector method, J. Water Resour. Plan. Manag. 144 (2018) 1–10, https://doi.org/10.1061/(asce)wr.1943-5452.0000798.
[31] S.S. Yang, S. Derakhshan, FY. Kong, Theoretical, numerical and experimental prediction of pump as turbine performance, Renew Energy 48 (2012) 507–513, https://doi.org/10.1016/j.renene.2012.06.002.